

## Use of Carbon Compounds (Carbon Nanotubes and Activated Carbon) in the Improvement of TiO<sub>2</sub>-Carbon Supercapacitor Performance

Joko Sudarto<sup>1\*</sup>, Agus Subagio<sup>1</sup>, Priyono<sup>1</sup>, Pardoyo<sup>2</sup>, R. Yudianti<sup>3</sup>, and Subhan<sup>4</sup>

1. Laboratory of Material Physics, Faculty of Mathematical and Natural Science, Universitas Diponegoro, Semarang 50275, Indonesia

2. Laboratory of Chemistry, Faculty of Mathematical and Natural Science, Universitas Diponegoro, Semarang 50275, Indonesia

3. Research Center for Physics, Indonesian Institute of Sciences, Bandung 40135, Indonesia

4. Research Center for Physics, Indonesian Institute of Sciences, Serpong 15314, Indonesia

\*E-mail: [joko@undip.ac.id](mailto:joko@undip.ac.id)

Received Februari 17, 2015 | Accepted November 21, 2016

### Abstract

Improvement of the performance of titanium oxide (TiO<sub>2</sub>)-carbon supercapacitor was studied by fabricating a double-layer electrode composite consisting of (TiO<sub>2</sub>), activated carbon (AC), and carbon nanotubes (CNTs). A thin layer of TiO<sub>2</sub>/CNT/AC electrode was coated on an aluminum foil substrate through the addition of a polyvinylidene fluoride adhesive of around 15% of the total weight of the composite. The resultant layer was then made into a double layer, and its conductivity and capacitance were measured using the electrochemical impedance spectroscopy (EIS). Results showed that the supercapacitor performance improved with the addition of CNTs. The highest performance was obtained with a composition of 23.3% TiO<sub>2</sub>, 21.0% CNT, and 4.0% AC with a  $1.29 \times 10^{-2}$  S/m conductivity and 5.56 F/g capacitance (C) at a frequency of 0.1 Hz.

### Abstrak

**Pengaruh Senyawa Karbon (Carbon Nanotube dan Activated Carbon) pada Peningkatan Kinerja Superkapasitor TiO<sub>2</sub>-Karbon.** Peningkatan kinerja superkapasitor TiO<sub>2</sub>-Karbon dipelajari dengan cara membuat komposit elektroda double-layer yang terdiri dari (TiO<sub>2</sub>), karbon aktif (AC), dan karbon nanotube (CNT). Lapisan tipis elektroda TiO<sub>2</sub>/CNT/AC dilapiskan pada substrat aluminium foil dengan penambahan perekat polyvinylidene fluoride sekitar 15% dari berat total komposit. Lapisan yang dihasilkan kemudian dibuat menjadi dua lapisan untuk kemudian konduktivitas dan kapasitansinya diukur menggunakan impedansi spektroskopi elektrokimia (EIS). Hasil penelitian menunjukkan bahwa kinerja super ditingkatkan dengan penambahan CNT. Kinerja tertinggi diperoleh dengan komposisi 23.3% TiO<sub>2</sub>, 21.0% CNT, dan 4.0% AC dengan nilai konduktivitas  $1.29 \times 10^{-2}$  S/m dan nilai kapasitansi 5.56 F/g pada frekuensi 0.1 Hz.

*Keywords: activated carbon, carbon nanotubes, supercapacitor, titanium oxide*

### Introduction

Electrical energy has become a basic human need, and many people take advantage of electronic equipment to support their activities. Technological development enables electronic devices to be easily adapted to human needs. Electronics devices are now portable without compromising their functionality. One drawback of their small shape is the reduced amount of electrical

storage. Therefore, the development of high-performance energy storage devices is urgent.

Electrical energy can be stored either in batteries or in capacitors. Batteries are the better option because they store a greater amount of energy than capacitors. Nevertheless, capacitors also have advantages, such as faster charging rate, shorter discharge time (0.3-30 seconds), and accommodation of greater power of more

than 1000 W/kg, thus making them a good alternative to batteries [1]. Capacitors with a large life cycle capability are also an attractive option as they last longer than batteries; batteries last 3-7 years, whereas supercapacitors can last up to 20 years [2].

The performance of supercapacitors is determined by the structural and electrochemical properties of the electrode [3]. These properties are evident in electrochemical capacitors, both in the pseudocapacitor and the electric double-layer capacitor types. The performance of electrochemical capacitors can be improved by applying metal oxides in the electrode. The application of ruthenium oxide ( $\text{RuO}_2$ ) provides high specific capacitance and power, but  $\text{RuO}_2$  is costly and toxic [4]. Therefore, many research groups focused on the other various metal oxides to replace  $\text{RuO}_2$  using  $\text{ZnO}$  [5,6], nickel oxide [7,8], cobalt oxide [9], or manganese oxide supercapacitors [10]. All of these metal oxides are inexpensive and exhibit pseudo capacitive behavior similar to that of  $\text{RuO}_2$ . Nanostructured metal oxides, which exhibit a pseudo capacitive behavior, are considered excellent materials for achieving high specific capacitance [11]. Recently, various other metal oxides that are less expensive and abundant in nature have been investigated [12]. Other composites containing  $\text{RuO}_2$  and carbon materials, such as carbon, carbon aerogels, carbon nanotubes (CNTs), and carbon nanofibers, have been intensively studied as supercapacitor materials [13,14]. Titanium oxide ( $\text{TiO}_2$ ) has been found to be one viable alternative. Titanium nanotubes are obtained by alkaline hydrothermal treatment [15,16].  $\text{TiO}_2$  is a good dielectric material and exhibits faradaic capacitance. Activated carbon (AC) has high specific surface area, good electrochemical stability, good conductivity, and high super capacity life cycle [17]. The combination of high surface area of AC and the large specific capacity of  $\text{TiO}_2$  forms a composite material with the properties of faradaic capacitance of the metal oxide and the double-layer capacitance of the AC [18].

In this study, we develop these composite materials by adding CNTs into electrodes. CNTs have the same behavior as AC but are better in terms of conductivity [19]. Electrodes that have been made to form  $\text{TiO}_2$ , AC, and CNTs with different ratios are measured using the electrochemical impedance spectroscopy (EIS) method.

## Experiment

Composites made of commercial AC and  $\text{TiO}_2$  (Sigma Aldrich) with additional multi-walled CNTs were fabricated. These materials were made into four compositions, the mass fractions of which are given in Table 1.

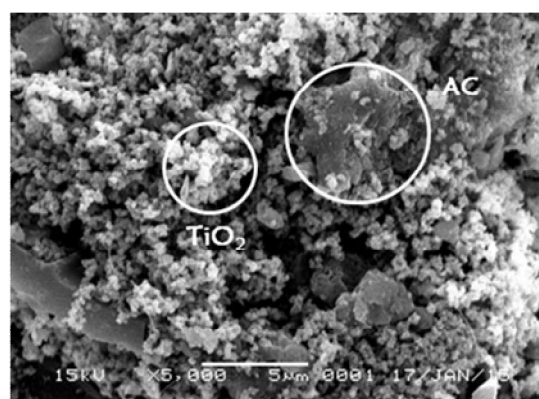
The subsequent step was testing the four samples using scanning electron microscopy (SEM) to determine the

composition of their morphology. Then, the samples were made into slurry using a conductive solution of polyvinylidene fluoride (PVDF), which had been previously dissolved in a dimethylacetamide solution with a 1:15 ratio.

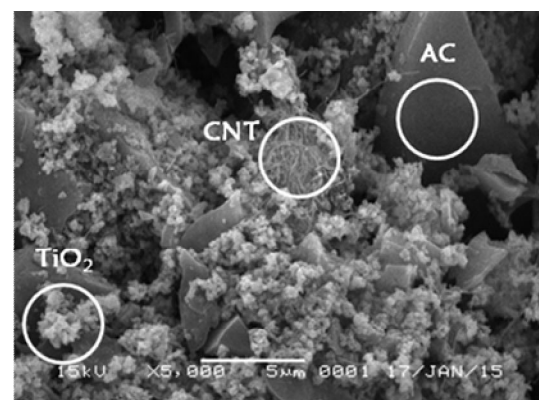
PVDF was prepared by heating it to a temperature of 50-80 °C while stirring for approximately 15-45 min. The PVDF solution was dripped slowly on the sample to form slurry that coats an aluminum foil. The coated aluminum foil was then dried and made into a double-electrode capacitance, which was divided by the Celgard separator and then later measured by EIS.

**Table 1. Mass Fractions of  $\text{TiO}_2$ , CNT, and AC**

Sample	Material	Mass Fraction
A	$\text{TiO}_2$ +AC	23.3% + 70%
B	$\text{TiO}_2$ +CNT+AC	23.3% + 7% + 63%
C	$\text{TiO}_2$ +CNT+AC	23.3% + 14% + 56%
D	$\text{TiO}_2$ +CNT+AC	23.3% + 21% + 49%



(a)



(b)

**Figure 1. SEM Images (A)  $\text{TiO}_2$ /AC with Mass Fractions of 23.3%:70% (without CNT) and (B)  $\text{TiO}_2$ /CNT/AC with Mass Fractions of 23.3%:21%:70%**

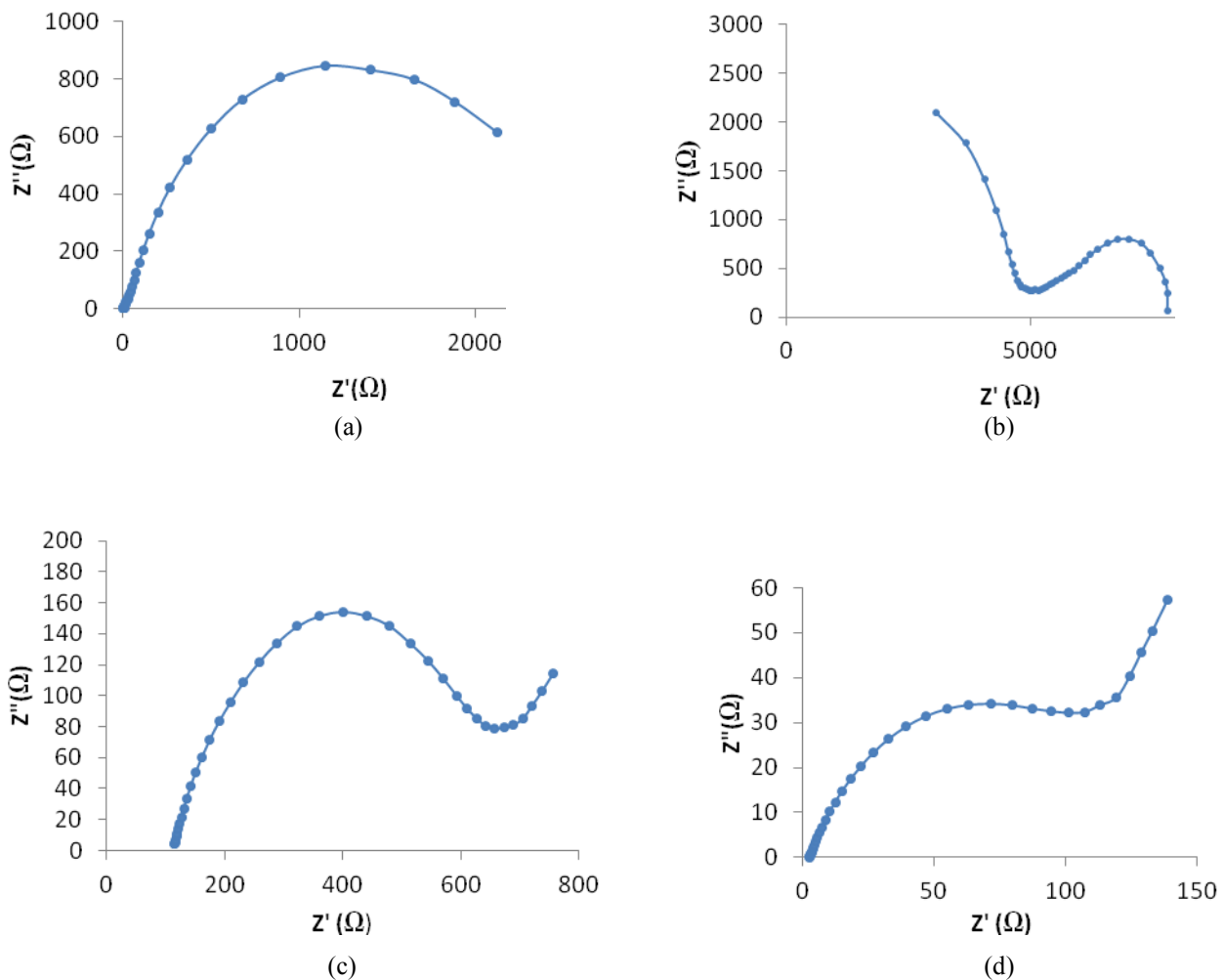


**Figure 2. Nyquist Plot of the Double-Layer Composite of TiO<sub>2</sub>/CNT/AC at A 0.1–100,000 Hz Frequency Range. The Mass Fractions are (a) Sample A, (b) Sample B, (c) Sample C, and (d) Sample D**

As indicated in Table 1, the composite powders of TiO<sub>2</sub>/CNT/AC were analyzed for their morphological characteristics using SEM (JEOL JED 2300 analyzer). This test was conducted to confirm the presence of each material and determine its distribution. Before the SEM analysis was performed, the sample was milled for 30 min. The SEM images are presented in Figure 1.

## Results and Discussion

In Figure 1, the SEM image shows that each material exists. Figure 1a illustrates the presence of AC in the form of chunks of black coral. TiO<sub>2</sub> is also visible, and some of it is covered by AC. In Figure 1b, sample D shows the presence of AC, TiO<sub>2</sub>, and CNTs in the form of long fibers. This observation proves that the composite powder does not experience any phase change. However, the image indicates that the mixing was uneven and therefore caused low homogeneity.

To minimize this heterogeneity, the composites were coated onto a 200  $\mu\text{m}$ -thick aluminum foil substrate. Once dry, this substrate formed a circular double electrode. These double electrodes were divided by the Celgard separator and wetted into the Na<sub>2</sub>SO<sub>4</sub> electrolyte.

The EIS method was used to measure the conductance and capacitance of this electrode. The Hioki 3522 LCR meter works at a frequency range of 0.1–100,000 Hz. The results of these measurements yielded values of the real ( $Z'$ ) and imaginary ( $Z''$ ) impedances.

These values were then represented in the Nyquist plot, which was used to analyze conductivity and capacitance. The Nyquist plot results are shown in Figure 2 for all samples. In the double-electrode measurements, the equivalent circuit that appears can be described as a simple parallel similar to a Randles cell. Therefore, the

equivalence of this circuit is always in semicircle form in the Cartesian coordinate.

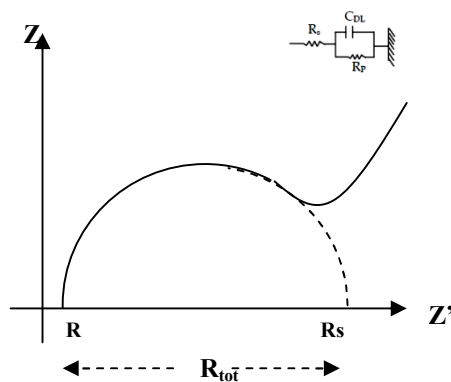


**Figure 3. Graphical Representation of One Semi-circle in a Parallel Circuit**

The semi-circle in Figure 3 can be determined from one simple parallel circuit of a capacitor-resistor. The semi-circle on the Nyquist plot can explain the charge transfer or polarization resistance that occurs in the electrode, where the resistance of an element is produced from the point of intersection at the x-axis (real impedance). The beginning of the semicircle line (left-intercept of  $Z''$  at the  $Z'$  axis) represents the resistance ( $R_s$ ) of the electrolyte in contact with the current collector and electrode. The termination of the semicircle line (right-intercept of  $Z''$  at the  $Z'$  axis) represents the internal resistance ( $R_p$ ) of the electrode. The diameter of the semicircle ( $R_p - R_s$ ) is equal to the  $R_{tot}$  value. The values of  $R_{tot}$  for all the samples determined from the data in Figure 2 are listed in Table 2.

As resistance is the inverse of conductance, the value of conductivity ( $\sigma$ ) can be obtained using Equation (1).

$$\sigma = \frac{l}{AR_{tot}} \tag{1}$$

where  $A$  is the area of the electrode and  $l$  is the thickness of the electrodes. Electrical conductivity is expressed in units of  $1/\Omega\text{m}$  (mho/m) or in Siemens/m (S/m). Bulk resistance ( $R_{tot}$ ) is obtained from the plot (Figure 3) by extrapolating the resultant graph into the semicircle.

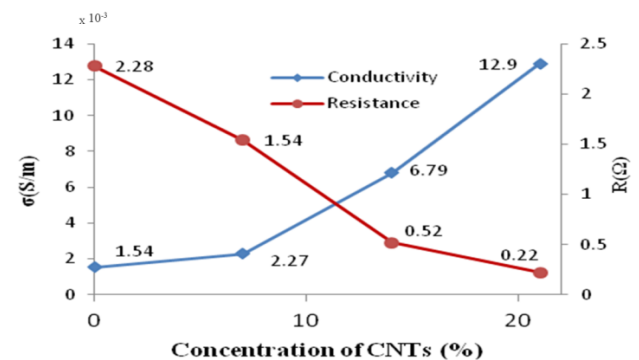
Treating the four samples of the Nyquist graph in Figure 2 in the same way reveals the conductivity of  $\text{TiO}_2/\text{CNT}/\text{AC}$ , as given in Table 2.

Table 2 shows an increasing trend in conductivity with the increase in CNT concentration. The resistance value generated in sample A (without CNTs) is large at  $2280.74\Omega$ .

Resistance values gradually decrease (conductivity gradually increases) when the concentration of CNTs

**Table 2. Resistance and Conductivity of  $\text{TiO}_2/\text{CNT}/\text{AC}$  Samples**

Sample	Resistance ( $\Omega$ )	Conductivity (S/m)
A	2280.74	$1.54 \times 10^{-03}$
B	1543.80	$2.27 \times 10^{-03}$
C	516.18	$6.79 \times 10^{-03}$
D	217.88	$1.29 \times 10^{-02}$



**Figure 4. Effect of CNT Concentration on Supercapacitor Conductivity**

increases by 7%, 14%, and 21%. When these concentrations are plotted into a graph (Figure 4), the influence of CNTs significantly increases its contribution to electrode conductivity.

Nyquist plots can also be used to calculate capacitance. Capacitance can be calculated from the value of imaginary impedance ( $Z''$ ) and the maximum working frequency on the impedance. By ignoring the small value of inductance and capacitance,  $C$  is assumed to be ideal. Therefore, capacitance  $C$  can be written as Equation (2).

$$C = \frac{1}{2\pi f Z_{immax}} \tag{2}$$

where  $C$  is capacitance in units of farads and frequency  $f$  is in hertz. Equation (2) shows that capacitance is strongly influenced by the magnitude and frequency of imaginary impedance.

Sample A (without CNTs) exhibits only one semicircle, with a maximum curvature of the imaginary impedance at  $847 \Omega$  at a frequency of 0.4 Hz. With the addition of CNTs, the maximum imaginary impedance decreases. Sample B, which has a 7% CNT concentration, shows a maximum imaginary impedance that decreases to  $800 \Omega$

at 0.8 Hz. These results are in contrast to those of samples C (CNT 14%) and D (CNTs 21%), which exhibit

**Table 3. Maximum Capacitance of TiO<sub>2</sub>/CNT/AC Samples**

Samples	C <sub>DL</sub> (F)	Mass (g)	C <sub>SP</sub> (F/g)
A (0% CNTs)	$0.26 \times 10^{-03}$	0.0174	0.03
B (7% CNTs)	$0.24 \times 10^{-02}$	0.0162	0.30
C (14% CNTs)	$1.39 \times 10^{-02}$	0.0142	1.96
D (21% CNTs)	$2.78 \times 10^{-02}$	0.010	5.56

an impedance of 154  $\Omega$  and 34.2  $\Omega$ , respectively. Therefore, if the imaginary impedance is small, capacitance increases, especially if the frequency bandwidth is not adequate.

As the samples are in a double layer, Equation (2) can be represented as a capacitance double-layer value. To obtain a specific capacitance for each gram, we use Equation (3):

$$C_{DL} = \frac{m.C_{sp}}{2} \quad (3)$$

Equation (3) can also be used to determine the capacitance of an Electric Double Layer Capacitor (EDLC) because C<sub>DL</sub> is already known from Equation (2), and the specific capacitance (C<sub>SP</sub>) can be calculated. The results of this specific capacitance calculation are presented in Table 3.

In the frequency range of 0.1-100,000 Hz, the highest capacitance is obtained for the CNT sample with the highest mass fraction (21%) at the lowest frequency of (0.1 Hz). Capacitance at this frequency reaches 5.56 F/g. The lowest capacitance value at the same frequency is 0.03 F/g with no additional CNTs. These results are far from the expected ones. However, the use of other methods, such as performing the pre-treatment procedure of CNTs or employing microwave heating, may obtain a better value of greater than 100 F/g [18, 20].

## Conclusion

Supercapacitor electrodes made of TiO<sub>2</sub>/CNT/AC composites are investigated using the EIS. The addition of CNTs with mass concentrations of 0%, 7%, 14%, and 21% indicates that the high-performance supercapacitors exhibited by the samples have high conductivity, with the largest CNT concentration at 21%. Moreover, the increase in CNTs also leads to a large capacitance. The TiO<sub>2</sub>/CNT/AC nanocomposite can be a potential candidate

for supercapacitor electrodes because of its efficiency, low cost, and simple methodology.

## Acknowledgments

This research was made possible by the assistance of experts at LIPI Serpong and at the Materials Physics Laboratory of Diponegoro University.

## References

- [1] Christen, T., Carlen, M.W. 2000. Theory of Ragone plots. *J. Power Source*. 91(2): 210-216, [http://dx.doi.org/10.1016/S0378-7753\(00\)00474-2](http://dx.doi.org/10.1016/S0378-7753(00)00474-2).
- [2] Sharma, P., Bhatti, T.S. 2010. A review on electrochemical double-layer capacitors. *Energy Conv. Manag.* 51(12): 2901-2912, <http://dx.doi.org/10.1016/j.enconman.2010.06.031>.
- [3] Burke, A. 2000. Ultracapacitors: Why, how, and where is the technology. *J. Power Sources*. 91(1): 37-50, [http://dx.doi.org/10.1016/S0378-7753\(00\)00485-7](http://dx.doi.org/10.1016/S0378-7753(00)00485-7).
- [4] Hu, C.C., Chen, W.C. 2000. Effects of substrates on the capacitive performance of RuOx·nH<sub>2</sub>O and activated carbon–RuOx electrodes for supercapacitors. *Electrochimica Acta*. 49(21): 3469–3477, <http://dx.doi.org/10.1016/j.electacta.2004.03.017>.
- [5] Kalpana, D., Omkumar, K.S., Sureshkumar, S., Renganathan, N.G. 2006. A novel high power symmetric ZnO/carbon aerogel composite electrode for electrochemical supercapacitor. *Electrochimica Acta*. 52(3): 1309-1315, <http://dx.doi.org/10.1016/j.electacta.2006.07.032>.
- [6] Jayalakshmi, M., Palaniappa, M., Balasubramanian, K. 2008. Single step solution combustion synthesis of ZnO/carbon composite and its electrochemical characterization for supercapacitor application. *Int. J. Electrochem. Sci.* 3: 96-103.
- [7] Hu, Y., Tolmachev, Y.V., Scherson, D.A. 1999. Rotating ring-disk studies of oxidized nickel hydroxide: oxygen evolution and pseudocapacitance. *J. Electroanal. Chem.* 468(1): 64-69, [http://dx.doi.org/10.1016/S0022-0728\(99\)00029-7](http://dx.doi.org/10.1016/S0022-0728(99)00029-7).
- [8] Lang, J.W., Kong, L.B., Wu, W.J., Liu, M., Luo, Y.C., Kang, L. 2009. A facile approach to the preparation of loose-packed Ni(OH)<sub>2</sub> nanoflake materials for electrochemical capacitors. *J. Solid State Electrochem.* 13: 333-340, doi:10.1007/s10008-008-0560-0.
- [9] Liang, Y.Y., Bao, S.J., Li, H.L. 2007. Nanocrystal line nickel cobalt hydroxides/ultrastable Y zeolite composite for electrochemical capacitors. *J. Solid State Electrochem.* 11(5): 571-576, doi: 10.1007/s10008-006-0197-9.
- [10] Amade, R., Jover, E., Caglar, B., Mutlu, T., Bertran, E. 2011. Optimization of MnO<sub>2</sub>/ vertically aligned carbon nanotube composite for supercapacitor application. *J. Power Sources*.

- 196(13): 5779-5783, <http://dx.doi.org/10.1016/j.jpowsour.2011.02.029>.
- [11] Xu, C.L., Bao, S.J., Kong, L.B. Li, H., Li, H.L. 2006. Highly ordered MnO<sub>2</sub> nanowire array thin films on Ti/Si substrate as an electrode for electrochemical capacitor. *J. Solid State Chem.* 179(5): 1351-1355, <http://dx.doi.org/10.1016/j.jssc.2006.01.058>.
- [12] Zheng, J.P. 2003. The Limitations of Energy Density of Battery/Double-Layer Capacitor Asymmetric Cells. *J. Electrochem. Soc.* 150(4): A484-A492, doi: 10.1149/1.1559067.
- [13] Arabale, G., Wagh, D., Kulkarni, M., Mulla, I.S., Vernekar, S.P., Vijayamohanam, K. Rao, A.M. 2003. Enhanced supercapacitance of multiwalled carbon nanotubes functionalized with ruthenium oxide. *Chem. Phys. Lett.* 376(1-2): 207-213, [http://dx.doi.org/10.1016/S0009-2614\(03\)00946-1](http://dx.doi.org/10.1016/S0009-2614(03)00946-1).
- [14] Kim, Y.T., Tadai, K., Mitani, T. 2005. Highly dispersed ruthenium oxide nanoparticles on carboxylated carbon nanotubes for supercapacitor electrode materials. *J. Mater. Chem.* 15: 4914-4921, doi: 10.1039/B511869G.
- [15] Seo, D.S., Lee, J.K., Kim, H. 2001. Preparation of nanotube-shaped TiO<sub>2</sub> powder. *J. Cryst. Growth.* 229(1-4): 428-432, [http://dx.doi.org/10.1016/S0022-0248\(01\)01196-4](http://dx.doi.org/10.1016/S0022-0248(01)01196-4).
- [16] Liu, X.M., Zhang, X.G. 2004. NiO-based composite electrode with RuO<sub>2</sub> for electrochemical capacitors. *Electrochimica Acta.* 49(2): 229-232, <http://dx.doi.org/10.1016/j.electacta.2003.08.005>.
- [17] Qinghan, M., Ling, L., Huaihe, S. 2004. Preparation and characterization of copper-activated carbon composite electrodes for supercapacitors. *J. Mater. Sci.* 39: 3149-3150, doi:10.1023/B:JMSC.0000025845.43085.d6.
- [18] Selvakumar, M., Bhat, D.K. 2012. Microwave synthesized nanostructured TiO<sub>2</sub>-activated carbon composite electrodes for supercapacitor. *Appl. Surface Sci.* 263: 236-241, <http://dx.doi.org/10.1016/j.apsusc.2012.09.036>.
- [19] Pan, H., Li, J., Feng, Y.P. 2010. Carbon Nanotubes for Supercapacitor. *Nanoscale Res. Lett.* 5: 654-668, doi: 10.1007/s11671-009-9508-2.
- [20] Hsieh, C., Huq, M.M. 2014. Microwave synthesis of titania-coated carbon nanotube composites for electrochemical capacitors. *J. Power Sources.* 269: 526-533, <http://dx.doi.org/10.1016/j.jpowsour.2014.07.037>.